

Bolometric correction factors for Active Galactic Nuclei

Hagai Netzer ¹*

¹*School of Physics and Astronomy, Tel-Aviv University, Tel-Aviv 69978, Israel*

24 July 2019

ABSTRACT

The bolometric luminosity of active galactic nuclei (AGN) is difficult to determine and various approximations have been used to calibrate it against different observed properties. Here I combine theoretical calculations of optically thick, geometrically thin accretion disks, and observed X-ray properties of AGN, to provide new bolometric correction factors (k_{BOL}) over a large range of black hole (BH) mass, accretion rate, and spin. This is particularly important in cases where the mass accretion rate cannot be determined from the observed spectral energy distribution, and in cases where luminosity-independent correction factors have been used. Simple powerlaw approximations of k_{BOL} are provided for $L(5100\text{\AA})$, $L(3000\text{\AA})$, $L(1400\text{\AA})$, $L(2\text{--}10\text{ keV})$ and $L(\text{narrow H}\beta)$. In all cases the uncertainties are large mostly due to the unknown BH spin. Prior knowledge of the BH mass reduces the uncertainty considerably.

Key words:

(galaxies:) quasars: general; galaxies: nuclei; galaxies: active; accretion, accretion discs

1 BACKGROUND

A major challenge in the study of active galactic nuclei (AGN) is the estimate of their bolometric luminosity (hereafter L_{AGN}). The main limitation is that much of the rest-frame ultraviolet (UV) spectral energy distribution (SED) is hidden from view, either due to galactic absorption in low redshift objects, or inter-galactic absorption in high redshift objects. Additional difficulties are the limited wavelength range accessible to various survey like SDSS, WISE and UKIDSS, the variability which is hard to measure, and dust extinction in some objects. The uncertain L_{AGN} affects the estimate of black hole (BH) growth and the Eddington ratio (L/L_{Edd}). It also limits our understand of the interaction of the central radiation source with the central accretion disk (AD), the broad line region (BLR), the narrow line region (NLR), the central dusty torus, the interstellar matter (ISM) in the host galaxy, and the inter-galactic medium at larger distances. These issues have been discussed in numerous publications (for recent reviews see Beckmann & Shrader 2012; Netzer 2013).

AGN are probably powered by the conversion of gravitational energy to electromagnetic radiation via various types of accretion flows. Examples of such flows are radiatively efficient, optically thick, geometrically thin ADs, (e.g. Shakura & Sunyaev 1973, hereafter SS73), radiatively inefficient, advection dominated accretion flows (ADAF, see e.g. Narayan 2005), and very high accretion rate, geometrically thick or slim disks (e.g. Mineshige et al. 2000; Sądowski & Narayan 2016). Radiatively efficient, geometrically thin ADs are perhaps the best understood accretion flows. Their

total radiative power is determined by the BH accretion rate (\dot{M}) and spin (represented by the spin parameter a), and their theoretical SEDs have been compared, successfully, with numerous observations. The mass to radiation conversion efficiency in such disks, η , ranges between 0.321 ($a = 0.998$) and 0.038 ($a = -1$). Perhaps the most detailed observations of such disks, in terms of rest-frame wavelength coverage, are those presented by Capellupo et al. (2015, 2016). They show a very good agreement between the predicted thin AD spectra and the observations. Various other publications, based on a more restricted wavelength range (see Davis et al. 2007; Jin et al. 2012a,b; Lusso et al. 2015), reach similar conclusions.

The higher accretion rate slim ADs are common but not so well understood. Such systems are identified either by their high normalized accretion rate \dot{M}/M_{BH} , or by their unique spectroscopic properties. Main candidates to host such disks are Narrow Line Seyfert 1 galaxies (NLS1s) or high redshift very luminous AGN, both with $L/L_{\text{Edd}} \sim 1$. There are attempts to calculate the SED of such sources using thin AD models with modified local temperature and opacity and various types of coronae (see e.g. Done et al. 2012, 2013; Kubota & Done 2018). Other models invoke saturated disk radiation above a certain L/L_{Edd} , due to radial advection, and/or powerful disk winds which are capable of carrying out a significant part of the released gravitational energy. Under these conditions, the connection between accretion rate, spin and radiated power, can differ substantially from those in thin ADs. The few available numerical calculations (e.g. Sądowski & Narayan 2016), suggest overall radiative efficiency which is lower than the efficiency of thin ADs, perhaps in the range 0.01–0.08.

The low efficiency flows, like ADAFs, are also less well

* E-mail: hagainetzer@gmail.com

understood. Here, again, there is no simple relationship between L_{AGN} , BH spin, and accretion rates, and η is low, perhaps below 10^{-3} . The present work focus on geometrically thin, optically thick ADs; the main power-house of most observed high ionization AGN, but perhaps not all LINERs.

Most AGN are powerful X-ray emitters with energy in the approximate range 0.2-100 keV, where the limit at 0.2 keV is arbitrarily determined by the capability of most X-ray instruments. In radio-quiet AGN, the emitted X-ray radiation is thought to be drawn, entirely, from the gravitational energy of the accretion flow. The origin of the X-ray radiation is still somewhat unclear. The soft X-ray radiation may be associated with a Compton thick medium at the surface of the disk (e.g. Done et al. 2012, and references therein). At higher energies, the emitted radiation is probably produced by a Compton thin corona which extends over the central parts of the disk (see e.g. Done et al. 2012; Reynolds 2016; Kubota & Done 2018). While not all the details of these processes are understood, the relations between the total X-ray luminosity L_X , (in this work the integrated 0.2-100 keV luminosity) and L_{AGN} , are well constrained, because these parts of the SED are readily accessible for X-ray instruments. In this paper I use the 2-10 keV energy, $L(2-10 \text{ keV})$, as a proxy for L_X .

Some of the emitted disk radiation can ionize low-density gas in the NLR which results in easy to observe narrow emission lines. The lines can be used to estimate L_{AGN} provided the gas is optically thick to Lyman continuum radiation, and its covering factor (C_f), and amount of dust extinction, are known. Detailed investigation of these issue have been published by Heckman et al. (2004), Netzer (2009), Heckman & Best (2014), and others.

The purpose of this paper is to calculate various optical, UV and X-ray bolometric correction factors (hereafter k_{BOL}) for AGN that are powered by optically thick, geometrically thin ADs that extend all the way to the innermost stable circular orbit (ISCO). It follows several earlier publications discussing this issue (e.g. Marconi et al. 2004; Vasudevan & Fabian 2007; Richards et al. 2006; Netzer 2009; Nemmen & Brotherton 2010; Runnoe et al. 2012a; Jin et al. 2012a; Trakhtenbrot & Netzer 2012; Krawczyk et al. 2013; Netzer et al. 2016). Improving the accuracy of such estimations is required in many cases where the accretion rate cannot be determined from the optical SED either because of the redshift or the very high luminosity of the sources (see e.g. Fig. 1 in Netzer & Trakhtenbrot 2014).

In §2 I describe the accretion disk and X-ray models and explore k_{BOL} over a large range of BH mass, spin, and accretion rate. In §3 I discuss the implications to AGN study and in §4 I summarize the results.

2 CALCULATIONS

This work provides theoretically-based calculations for a variety of bolometric correction factors: $k_{\text{BOL}}(5100\text{\AA})$, $k_{\text{BOL}}(3000\text{\AA})$, $k_{\text{BOL}}(1400\text{\AA})$, $k_{\text{BOL}}(2-10 \text{ keV})$ and $k_{\text{BOL}}(\text{narrow H}\beta)$, where $L_{\text{AGN}}=k_{\text{BOL}} \times (\text{observed luminosity})$ and $L(1400\text{\AA})$ stands for λL_λ at 1400Å. The calculations are limited to optically thick, geometrically thin ADs assuming that accretion through the disk, with time independent accretion rate, is the only energy production mechanism. and $L_{\text{AGN}}=\eta\dot{M}c^2$. For reasons explained below, I avoid slim accretion disks with $L/L_{\text{Edd}} > 0.5$. I also avoid very low accretion rate systems, with $L/L_{\text{Edd}} < 0.001$. The emitted X-ray radiation is assumed to be drawn from the same source of energy, thus the calculated L_X does not affect the derived L_{AGN} . The range of BH mass

is $10^7 - 10^{10} M_\odot$, and the BH spin parameter covers the entire range allowed for such systems, from -1 to 0.998.

2.1 Accretion disk calculations

The accretion disk model used here is described in Slone & Netzer (2012). It is similar to the standard SS73 disk but includes also full relativistic corrections and Comptonization in the disk atmosphere. The disk is assumed to be stationary with a constant viscosity parameter $\alpha = 0.1$. It extends from the ISCO out to $r = 2160r_g$, where r_g is the gravitational radius. The calculations start with an assumed BH mass, BH spin and disk inclination. The entire SED is then calculated for a range of accretion rates such that the entire allowed range of L/L_{Edd} is covered. The resulting spectra are used to define $k_{\text{BOL}}(1400\text{\AA})$, $k_{\text{BOL}}(3000\text{\AA})$ and $k_{\text{BOL}}(5100\text{\AA})$.

Several other types of AGN disks have been considered. In particular, two or three-part disks involving warm and hot X-ray gas, have been suggested (e.g. Done et al. 2012; Kubota & Done 2018; Panda et al. 2019, and references therein). Such systems produce significantly different ionizing SEDs and are discussed, briefly, in §2.2. The code *QSOSED* is available as a part of *XSPEC* for calculating such SEDs.

The disk inclination factor assumed in the calculations takes a simple, wavelength-independent form.

$$\frac{L_v}{L_v(\text{face-on})} = \frac{1}{1+b} \cos\theta(1+b\cos\theta) \quad (1)$$

where θ is the inclination to the line of sight and b a limb darkening factor. The case $b = 0$ corresponds to the simplest case of $L_v \propto \cos\theta$. Here I use $b = 2$ which is in good agreement with an electron scattering atmosphere. There are some differences between the two assumed values of b regarding the dependence of the inferred k_{BOL} on the (observationally unknown) disk inclination. For type-I AGN, with $\cos\theta \sim 0.7$, they amount to only a few percent. For very large inclinations, those hardly observed in type-I sources, they are much larger. The values of $k_{\text{BOL}}(1400\text{\AA})$, $k_{\text{BOL}}(3000\text{\AA})$ and $k_{\text{BOL}}(5100\text{\AA})$ were calculated for a disk inclination that recovers the correct L_{AGN} by integrating L_v over the observed SED ($\theta \approx 56$ degrees).

As shown in Slone & Netzer (2012), and also in Laor & Davis (2014), disk winds can reduce L_{AGN} , soften the emitted spectrum and affect k_{BOL} . Such winds are not considered in this work. I also do not consider various line and bound-free absorption properties in the disk atmosphere that can significantly alter the far-UV SED (see e.g. Davis & Laor 2011) but not the total emitted power. As shown below, earlier calculations of k_{BOL} for geometrically thin ADs, by Nemmen & Brotherton (2010), resulted in bolometric correction factors similar to the ones presented here.

GR effects change photon trajectories close to the ISCO. For the BH mass in question, such effects are only noticeable at very large disk inclination and high spin (see e.g. Laor et al. 1990; Campitiello et al. 2018). Very few, if any type-I AGN are observed at such inclination angles. In addition, the angular radiation pattern of the X-ray source can be different from that of the geometrically thin AD. This can have important observational consequences (Netzer 1987) but is beyond the scope of the present work.

For illustration purpose, I only show four values of the spin parameter: -1, 0, 0.7 and 0.998. The corresponding mass-to-radiation conversion deficiencies are 0.038, 0.057, 0.104 and 0.321. I also show only four values of BH mass, $10^7 M_\odot$, $10^8 M_\odot$, $10^9 M_\odot$, and $10^{10} M_\odot$. This combination of BH mass and spin is enough to illustrate the entire range of k_{BOL} . I exclude cases where the

fractional ionizing luminosity is below 5%. For smaller fractions, the resulting equivalent width (EW) of the strongest broad emission lines are too small to be detected in big spectroscopic surveys, like SDSS. Such objects would normally not be classified as type-I AGN because of their very weak, small EW broad emission lines (see Laor & Davis 2011; Hryniewicz et al. 2010; Netzer & Trakhtenbrot 2014; Bertemes et al. 2016).

The transition between thin and slim accretion disks depends on $\dot{M}/\dot{M}_{\text{BH}}$ which, for thin ADs, is proportional to L/L_{Edd} . The number chosen here, $L/L_{\text{Edd}}=0.5$, is somewhat arbitrary mostly because slim disk calculations are still rather uncertain. Proposed numbers range from $L/L_{\text{Edd}}=0.1$ to $L/L_{\text{Edd}}\approx 1$ (e.g. Sądowski et al. 2011; Du et al. 2015; Sądowski & Narayan 2016, and references therein). The transition to ADAF is taken to be $L/L_{\text{Edd}}=0.001$. This is also model dependent and several calculations assume lower values (see Sądowski & Gaspari 2017, and references therein). This limit leaves many LINERs outside the population considered here. As explained below, various other constraints further reduce the range of L/L_{Edd} .

2.2 X-ray calculations

The X-ray properties of AGN have been studied, extensively, in numerous papers (Vasudevan & Fabian 2007; Done et al. 2012, 2013; Jin et al. 2012b; Reynolds 2016; Kubota & Done 2018; Panda et al. 2019, and references therein).

X-ray production must be related to gas with a temperature significantly above the standard thin disk temperature. Several recent studies (e.g. Kubota & Done 2018; Panda et al. 2019) consider this radiation to originate from the regions nearest to the BH. These are divided into *warm corona*, producing the so-called “soft X-ray excess”, and *hot corona* producing the X-ray power-law. The fraction of the accretion energy dissipated in the two regions depends both on the accretion rate and the Eddington ratio.

Here I take a purely observational approach and consider only the hard X-ray power-law sources, with $N_E \propto E^{-\Gamma}$, where N_E is the photon flux at energy E chosen here to extend from 0.2 to 100 keV. In most AGN $1.6 < \Gamma < 2.2$ and the value itself must be related to the details of the accretion process. The value adapted here, $\Gamma = 1.9$, is representative of the population of radio quiet AGN (Ricci et al. 2017, and references therein). This slope results in $L_X=3.9L(2-10 \text{ keV})$ where $L_X=L(0.2-100 \text{ keV})$.

A central assumption of this work is the existence of a tight correlation between the UV and X-ray luminosities. This correlation, or its equivalent, α_{OX} , have been studied in numerous papers (e.g. Just et al. 2007; Jin et al. 2012b, and references therein). The form used here is adapted from the various fits presented in Lusso & Risaliti (2016) and is given by:

$$\log L_{\nu(2\text{keV})} = 0.62 \log L_{\nu(2500\text{\AA})} + 7.77 . \quad (2)$$

The measured scatter around this relationship depends on the X-ray slope Γ , on the (unknown) disk inclination, and on the way used to model the observed flux at 2500Å which is contaminated by broad FeII lines and Balmer continuum emission (see Mejía-Restrepo et al. 2016, and references therein).

Two general assumptions related to the X-ray radiation are used: 1) Full energy conservation (the radiated X-ray energy is drawn from the gravitational energy of the flow). 2) The production of X-ray photons does not affect *the measured* $L(5100\text{\AA})$, $L(3000\text{\AA})$ and $L(1400\text{\AA})$. The second assumption requires some justification.

As explained, the hard X-ray radiation is probably the results

of a hot, Compton-thin corona covering the central part of the disk and up-scatters the optical-UV continuum photons. Energetically, this involves heating of the corona, through dissipation, and changing the energy of the scattered radiation. Unlike the three region disks considered by Kubota & Done (2018), the disks in this work extend all the way to the ISCO. In this case, heating the corona can be achieved if a small fraction of the accretion flow, goes through the top layer of the disk and heats it to temperatures far above the thin AD temperature. This dissipation reduces the optical-UV luminosity compare with a case of a thin AD without a corona. If the corona covers only the innermost part of the disk, where most of the emitted flux is beyond 1 Rydberg, then the $E < 1$ Rydberg radiation, including $L(5100\text{\AA})$, $L(3000\text{\AA})$ and $L(1400\text{\AA})$, is not affected much by the entire process. Moreover, in this case most of the upscattered photons are Lyman continuum photons. Under such conditions, $L_X < L_{\text{ION}}$, where L_{ION} stands for the $E > 1$ Rydberg luminosity of a disk with the same accretion rate but without a corona. Since low spin, low accretion rate and large BH mass result in small $L_{\text{ION}}/L_{\text{AGN}}$, and L_X is assumed to depend directly on $L(2500\text{\AA})$ (eqn. 2), in some of these cases L_X can be large even when $L_{\text{ION}}/L_{\text{AGN}}$ is very small. Under such conditions, the lowest L/L_{Edd} that can be achieved is about 0.007, rather than the general low limit of 0.001 imposed earlier.

The alternative is a larger corona that extends far beyond the ISCO. In this case, there is a direct link between the $E < 1$ Rydberg radiation and L_X since the flow going through the corona reduces the emission from the parts of the disks where this radiation is emitted. Moreover, some of these photons are converted to X-ray radiation. This requires to impose a second condition of $L_X < 0.5L_{\text{AGN}}$. There are only a few known AGN where L_X is larger than the second limit.

All the calculations presented in this work apply to both conditions, $L_X < L_{\text{ION}}$ and $L_X < 0.5L_{\text{AGN}}$. For a detailed discussion of various possible geometries and types of coronae see Done et al. (2012) and Kubota & Done (2018).

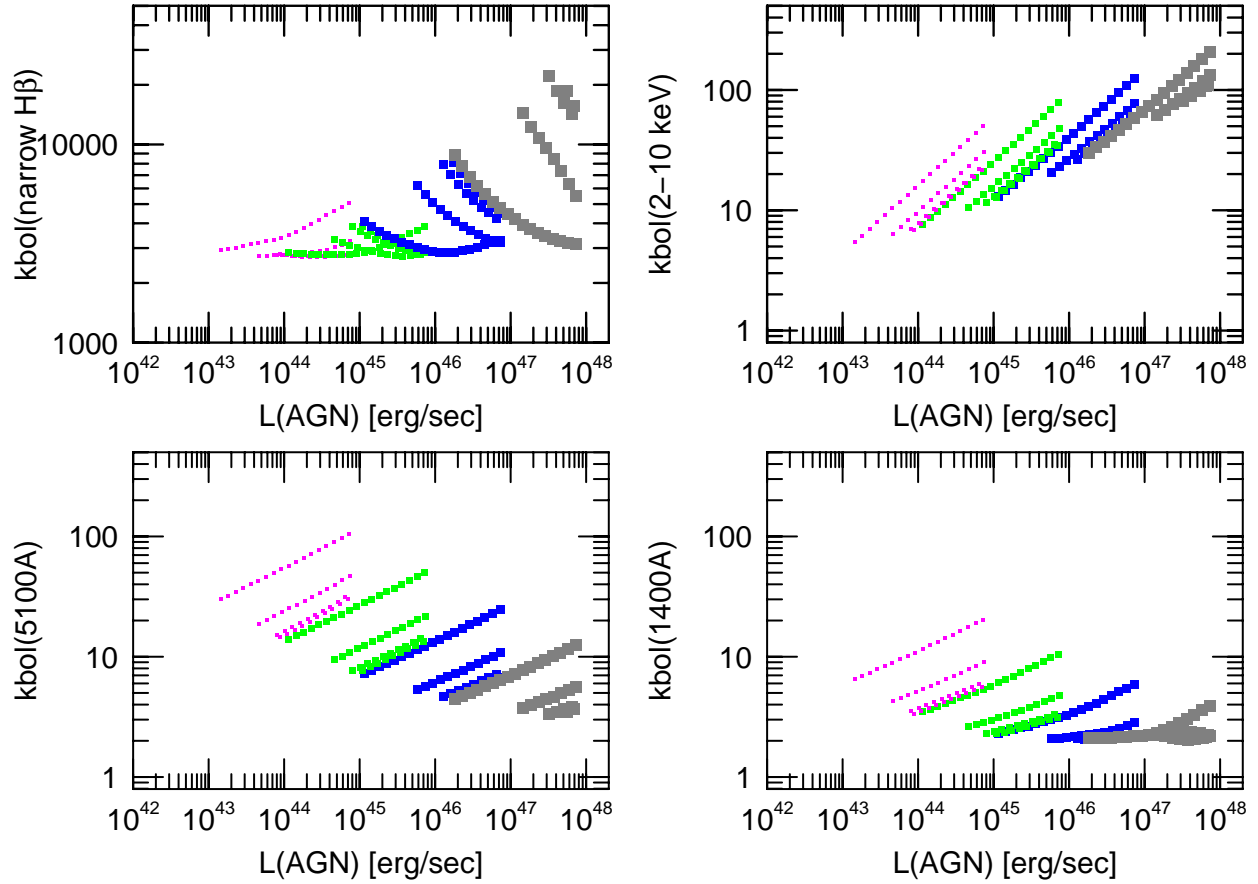


Figure 1. Various bolometric correction factors vs. L_{AGN} for thin accretion disks with “mean inclination” and X-ray properties as defined in this work. Here and in all other diagrams, point size represent BH mass. $M_{\text{BH}}=10^7 M_{\odot}$ (tiny points), $M_{\text{BH}}=10^8 M_{\odot}$ (small points), $M_{\text{BH}}=10^9 M_{\odot}$ (large points) and $M_{\text{BH}}=10^{10} M_{\odot}$ (largest points). Each BH mass is separated into four groups of spins: $a=-1$ (smallest k_{BOL}), $a=0$, $a=0.7$ and $a=0.998$ (largest k_{BOL}). The top left panel shows $k_{\text{BOL}}(\text{narrow H}\beta)$ assuming optically thick NLR with a covering factor of 0.05 and no internal dust.

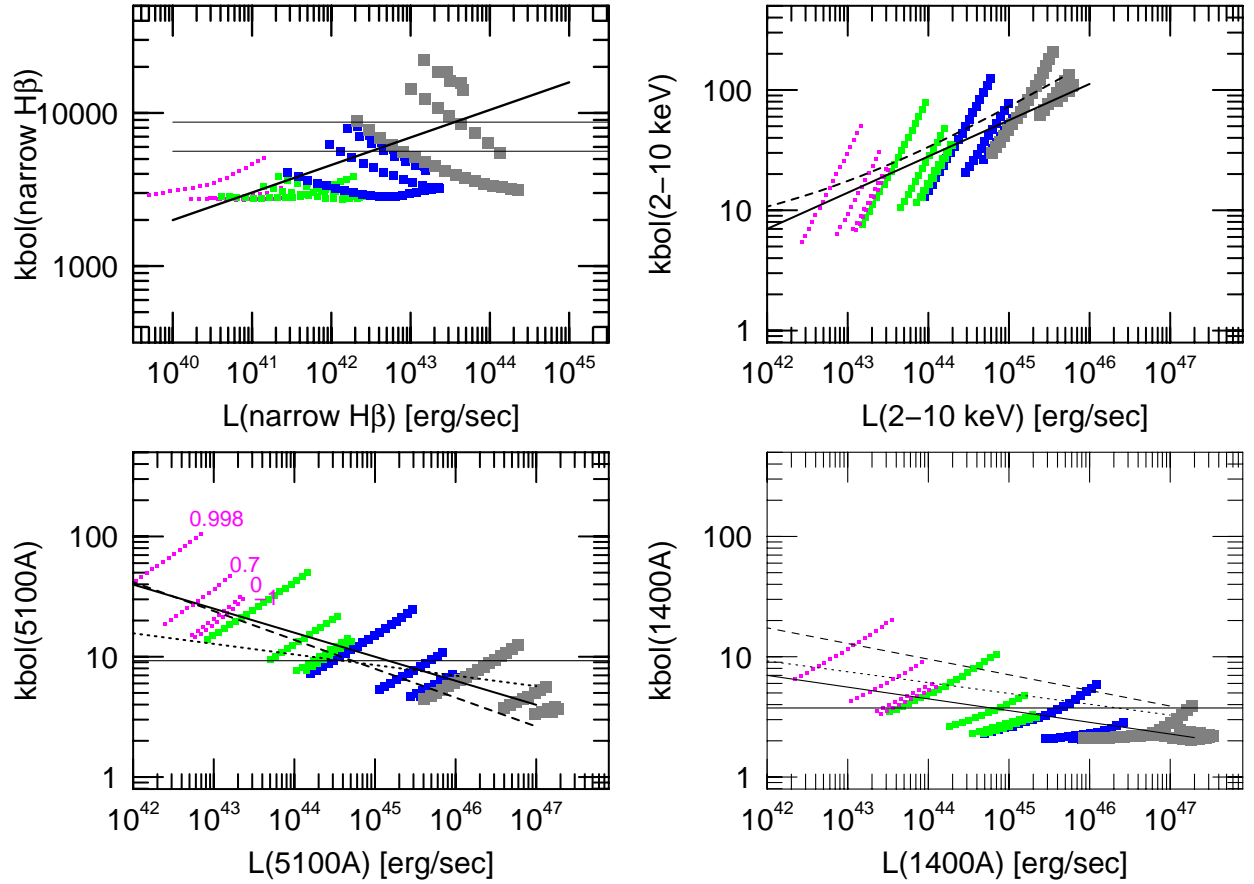


Figure 2. As Fig. 1 but for observed luminosities, as marked on the horizontal axis. The spin parameters (a) for $M_{\text{BH}}=10^7 M_{\odot}$ are marked in the bottom left panel. The black solid diagonal lines in all panels show the eye-fitted approximations given in eqn. 3 and Table 1. For $k_{\text{BOL}}(1400\text{\AA})$ and $k_{\text{BOL}}(5100\text{\AA})$ I also show the AD-based fit of Nemmen & Brotherton (2010) (dashed black lines), the expression derived for the power-law continuum by Runnoe et al. (2012a) (dotted black lines), and the constants used in the Shen et al. (2011) catalog following the Richards et al. (2006) analysis (solid black horizontal lines). The range marked by the two horizontal lines in $k_{\text{BOL}}(\text{narrow H}\beta)$ is the one recommended in Netzer (2009). For $k_{\text{BOL}}(2\text{-}10\text{ keV})$, the dashed black line is the Marconi et al. (2004) approximation.

2.3 Narrow emission line calculations

Several narrow emission lines have also been used to estimate L_{AGN} . The most useful ones are $\text{H}\alpha$, $\text{H}\beta$, $[\text{O III}] \lambda 5007$, and $[\text{O I}] \lambda 6300$ (see Netzer 2009; Heckman & Best 2014; Pennell et al. 2017, and references therein). In the present study, the Balmer line luminosities were calculated from the number of ionizing photons, assuming a nominal covering factor (C_f) for the NLR and a standard Case-B recombination with $T_e = 10^4 \text{K}$. Since $L(\text{narrow H}\alpha)/L(\text{narrow H}\beta)$ is known from recombination theory, I only show $k_{\text{BOL}}(\text{narrow H}\beta)$. Realistic photoionization calculations must also take into account the fraction of ionizing radiation absorbed by dust grains and hence not available for ionizing hydrogen. The exact fraction depends mostly on the ionization parameter (U) of the NLR gas (see Netzer 2013). The results shown below assume $C_f=0.05$ and no dust absorption. This tends to overestimate the $L(\text{narrow H}\beta)$, especially for $U > 10^{-2}$.

The calculations of $L([\text{O III}] \lambda 5007)$ are more problematic. The line luminosity is sensitive to both the shape of the ionizing SED (known in this work) and the ionization parameter (not included in this work), and to a lesser extent on the gas metallicity. Two cases were considered: line luminosity which is scaled to L_{ION} , and line luminosity which is scaled to $L(E > 35.1 \text{ eV})$, where 35.1 eV is the ionization potential of O^+ . Both approximations are problematic because not all Lyman continuum photons can ionize O^+ , and because of the possible modification of the disk ionizing SED by soft X-ray radiation (e.g. Panda et al. 2019). A reasonable approximation is $L([\text{O III}] \lambda 5007)=0.0025(C_f(\text{NLR})/0.05)L_{\text{ION}}$ but this may fail at extreme cases of very large BH mass or very small BH spin, where $L(E > 35.1 \text{ eV})$ is very small. Because of this ambiguity, I do not provide calculated $k_{\text{BOL}}([\text{O III}] \lambda 5007)$ in this work.

Finally, $L([\text{O I}] \lambda 6300)$ is even more model dependent and no attempt was made to calculate $k_{\text{BOL}}([\text{O I}] \lambda 6300)$. Detailed photoionization calculations, and full discussion of these issues, including a comparison with a large sample of type-II AGN, are given in Netzer (2009).

2.4 Bolometric correction factors

The calculations of the various bolometric correction factors are presented in Fig. 1 and Fig. 2. The bottom part of Fig. 1 shows the correlation of $k_{\text{BOL}}(5100\text{\AA})$ and $k_{\text{BOL}}(1400\text{\AA})$ with L_{AGN} . There are four colors and point sizes that represent four BH masses: $M_{\text{BH}}=10^7 M_{\odot}$ (tiny points), $M_{\text{BH}}=10^8 M_{\odot}$ (small points), $M_{\text{BH}}=10^9 M_{\odot}$ (large points) and $M_{\text{BH}}=10^{10} M_{\odot}$ (largest points). Each of the mass groups is divided into four groups of spin parameter: -1 (lowest luminosity points), 0, 0.7, and 0.998 (highest luminosity points). Each group of colored points shows a rise from bottom left to upper right following the increase in mass accretion rate, \dot{M} . Since the behaviour of $k_{\text{BOL}}(3000\text{\AA})$ is in between the other two, I chose not to show it in a separate panel. It is important to emphasize that $k_{\text{BOL}}(3000\text{\AA})$ refers to the disk SED. In many AGN (see e.g. Mejía-Restrepo et al. 2016), the so-called “small blue bump” (a blend of Balmer continuum and FeII line emission) gives an impression of a local continuum which may be as large as 20-50% of the disk continuum. This must be taken into account when using this bolometric correction factor to find L_{AGN} .

The top panels of Fig. 1 and Fig. 2 show $k_{\text{BOL}}(2-10 \text{ keV})$ and $k_{\text{BOL}}(\text{narrow H}\beta)$. It is evident that the scatter in all diagrams is very large because of the large range in accretion rate and BH spin.

Table 1. Fitting constants for $k_{\text{BOL}}=c \times [L(\text{observed})/10^{42} \text{ erg/sec}]^d$ assuming “mean” disk inclination. The number in parentheses is for cases where the Balmer continuum and the FeII lines are included in $L(3000\text{\AA})$.

$L(\text{observed})$	c	d
$L(5100\text{\AA})$	40	-0.2
$L(3000\text{\AA})$	25(19)	-0.2
$L(1400\text{\AA})$	7	-0.1
$L(2-10 \text{ keV})$	7	0.3
$L(\text{narrow H}\beta)$	4580	0.18

The scatter in $k_{\text{BOL}}(2-10 \text{ keV})$ is somewhat smaller, mostly because this correction factor increases with L_{AGN} .

The calculations shown in Fig. 1 do not provide a practical way to estimate L_{AGN} . Therefore, I present in Fig. 2 the calculated k_{BOL} as a function of measured luminosities: $L(1400\text{\AA})$, $L(5100\text{\AA})$, $L(2-10 \text{ keV})$ and $L(\text{narrow H}\beta)$. I also present eye-fitted log-log lines that go roughly through the points. The purpose is to properly represent the case with $a = 0.7$ ($\eta = 0.104$) and hence the curves under-estimate k_{BOL} for the highest \dot{M} , maximum BH spin cases.

The simplified eye-fitted curves shown in Fig. 2 are given by:

$$k_{\text{BOL}} = c \times [L(\text{observed})/10^{42} \text{ erg/sec}]^d, \quad (3)$$

where $L(\text{observed})$ is the luminosity in question. Table 1 presents recommended values for the constants c and d . For the constant c in the expression for $k_{\text{BOL}}(3000\text{\AA})$ I give two approximations: one relative to the accretion disk continuum and one, in parentheses, for a case where the Balmer continuum and FeII line blends are not removed prior to the estimate of L_{AGN} .

There is no simple way to estimate the uncertainties in k_{BOL} since the number of points shown in the various diagrams has nothing to do with the distribution of BH mass, spin, and accretion rate in the AGN population. Moreover, the extreme values of k_{BOL} depend on the various constraints imposed here on L/L_{Edd} , $L_{\text{ION}}/L_{\text{AGN}}$ and $L_{\text{X}}/L_{\text{ION}}$. Fitting more sophisticated functions to these points, or using a χ^2 -type analysis is, therefore, not very meaningful. Perhaps a more meaningful way is to consider the extreme values of the various calculated k_{BOL} . This shows that, within the above constraints, the range is typically as large as the range in the mass conversion efficiency η (a factor of ~ 8.4) with some cases exceeding an order of magnitude. The range is considerably reduced at the high luminosity end where other considerations, such as the fraction of ionizing radiation, limit the observable properties.

Fig. 3 provides more information about the range of $k_{\text{BOL}}(5100\text{\AA})$ for the case of $M_{\text{BH}}=10^9 M_{\odot}$. The diagram shows the spin parameters considered earlier for various limits imposed by L_{ION} and L_{X} . The solid lines show the boundaries of the allowed region for $L_{\text{ION}} > 0.05 L_{\text{AGN}}$ and $L_{\text{X}} < L_{\text{ION}}$, the same as in Fig. 1 and Fig. 2. The boundaries are set by the smallest ($a = -1$) and largest ($a = 0.998$) BH spins, and by the smallest and largest L/L_{Edd} which are consistent with these conditions. While the upper limit of $L/L_{\text{Edd}}=0.5$ is reached for all values of a , the lowest Eddington ratio in this case (about 0.007) is much larger than the allowed lowest value of 0.001 (also shown in the diagram). This was obtained by changing the condition on L_{X} to be $L_{\text{X}} < 0.5 L_{\text{AGN}}$, which allows smaller values of L/L_{Edd} , in some cases as small as 0.001 (shown as a dashed line). The thick solid line marks the approximation of eqn. 3, as in Fig. 2. For the default case where $L_{\text{X}} < L_{\text{ION}}$, the uncertainty on L_{AGN} range from ± 0.05 dex to ± 0.35 dex, depending on $L(5100\text{\AA})$. Clearly, prior knowledge of M_{BH} can significantly improve the determination of L_{AGN} .

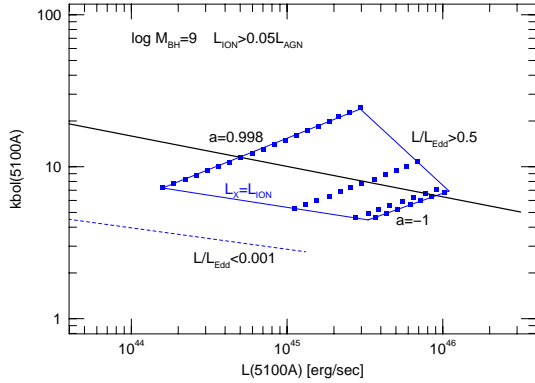


Figure 3. Boundaries for $k_{\text{BOL}}(5100\text{\AA})$ for the case of $M_{\text{BH}} = 10^9 M_{\odot}$. The boundaries set by the BH spin are marked by the spin parameter a . The region on the right is not allowed since $L/L_{\text{Edd}} > 0.5$ and the region below the lowest dashed line is where $L/L_{\text{Edd}} < 0.001$. The thick solid line is the approximation of eqn. 3.

Of the few earlier estimates of k_{BOL} , those of Nemmen & Brotherton (2010) and Runnoe et al. (2012a,b) are most relevant to this work. The Nemmen & Brotherton (2010) paper made use of a library of accretion disk SEDs computed by Hubeny and collaborators. While these models are superior to the disk models used here, the differences regarding k_{BOL} are very small. The best fit approximation recommended by the authors is shown by a dashed black line in Fig. 2. This line is similar to the eye-fitted approximation of the present work (note that Nemmen and Brotherton calculated $k_{\text{BOL}}(1450\text{\AA})$ which is practically identical to $k_{\text{BOL}}(1400\text{\AA})$ considered here). The expression obtained by Nemmen & Brotherton (2010) is based on a χ^2 method applied to a library of AD models with various mass, spin and accretion rate. It depends on the availability of such models and not on population properties, and is hence not superior to the eye-fitted curve used here.

Runnoe et al. (2012a) used a broken power-law SED, extending to 8 keV, to calculate a different set of bolometric correction factors. This is also shown in Fig. 2 by a dotted black line. Since the broken power-law continuum was chosen to correctly connect the optical and X-ray points, the resulting k_{BOL} is not very different from the ones computed here. Fig. 2 also shows the constant $k_{\text{BOL}}(5100\text{\AA})$ and $k_{\text{BOL}}(1350\text{\AA})$ used in the Shen et al. (2011) AGN catalog as adapted from the analysis in Richards et al. (2006).

I also show in Fig. 2 the widely used approximation of Marconi et al. (2004) which agrees with the AD approximation very well assuming $L_X < L_{\text{ION}}$. For the alternative possibility of $L_X < 0.5L_{\text{AGN}}$ (not shown here), the eye-fitted line would move down by about 0.3 dex. As shown by Vasudevan & Fabian (2007), and also by Jin et al. (2012b), the Marconi et al. (2004) approximation gives too small $k_{\text{BOL}}(2-10 \text{ keV})$ for NLS1s which is not surprising as such objects do not obey the basic relationship (eqn. 2) between $L(2500\text{\AA})$ and $L_{\text{V}(2\text{keV})}$ assumed here. The reason may be related to the type of ADs powering such sources (probably slim ADs with large L/L_{Edd}). Because of this, $k_{\text{BOL}}(2-10 \text{ keV})$ estimated here should not be used to estimate L_{AGN} in NLS1s.

Finally, the new calculations can be compared to those presented in Netzer (2009) where the recommended numbers for $k_{\text{BOL}}(\text{narrow H}\beta)$, assuming galactic-type extinction, is in the

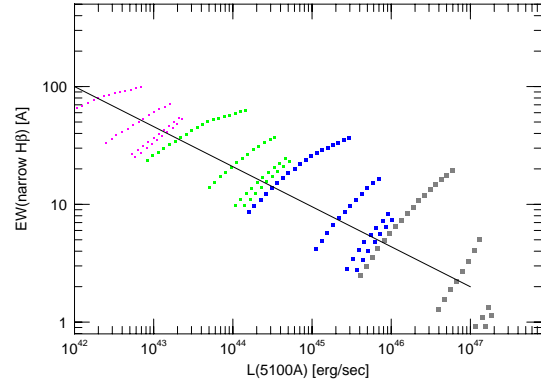


Figure 4. Calculated $\text{EW}(\text{narrow H}\beta)$ for thin ADs assuming $C_f=0.05$ and no absorption of ionizing radiation by dust grains inside the NLR clouds.

range 5600-8700 (shown in Fig. 2), for $L([\text{O III}] \lambda 5007)/L(\text{narrow H}\beta) < 12$. The new results are in reasonable agreement with this estimate especially given the uncertain amount of ionizing radiation absorbed by dust grains and the scatter in covering factor. The reason for the large increase in $k_{\text{BOL}}(\text{narrow H}\beta)$ at high $L(\text{narrow H}\beta)$ is the decrease in $L_{\text{ION}}/L_{\text{AGN}}$ at the high mass end.

The new models can be used to calculate $\text{EW}(\text{narrow H}\beta)$ using the computed $L(5100\text{\AA})$ and $L(\text{narrow H}\beta)$. This is shown in Fig. 4. The numbers can be compared with observations of type-I AGN with little or no dust reddening of the disk continuum. A simple eye-fitted curve gives: $\text{EW}(\text{narrow H}\beta) = 100(C_f(\text{NLR})/0.05)[L(5100\text{\AA})/10^{42}]^{-0.34}$. As noted earlier, the calculations are not suitable for estimating the $[\text{O III}] \lambda 5007$ luminosity and hence also not for estimating $\text{EW}([\text{O III}] \lambda 5007)$. Some idea of the oxygen line luminosity and equivalent width can be obtained by noting that most type-II AGN fall in the range $2 < L(\text{narrow } [\text{O III}] \lambda 5007)/L(\text{narrow H}\beta) < 10$ where high ionization AGN occupy the upper part and LINERs the lower part of this range.

3 IMPLICATIONS TO AGN STUDY

The calculations presented here illustrate the big uncertainties associated with the estimate of L_{AGN} using bolometric correction factors based on various measured luminosities. Several commonly used estimates provide reasonable approximations to the mean population properties but can be wrong, by an order of magnitude or more, for individual sources. BH mass estimates can significantly improve this situation (see Fig. 3). In addition, in low redshift, low luminosity type-I AGN, where the part of the SED with $L_{\text{nu}} \propto \nu^{1/3}$ is directly observed, \dot{M} can be estimated from the luminosity of the long wavelength continuum (e.g. Collin et al. 2002; Laor & Davis 2011; Netzer & Trakhtenbrot 2014). In such cases, the combination of M_{BH} and \dot{M} limit the uncertainty to the unknown BH spin and measuring optical, UV or X-ray luminosity can reduce it further.

For type-I AGN, the unknown disk inclination is another source of uncertainty. All the calculations presented here are for an inclination of ~ 56 degrees. For a torus covering factor of 0.5, the mean expected inclination is smaller, corresponding to $\cos \theta \sim 0.7$. This would over-estimate the disk luminosity by a factor of ~ 1.4 and requires a corresponding decrease in $k_{\text{BOL}}(1400\text{\AA})$,

$k_{\text{BOL}}(3000\text{\AA})$ and $k_{\text{BOL}}(5100\text{\AA})$. For face-on ADs, the number is closer to 2.5.

An interesting feature in Fig. 2 is the convergence of $k_{\text{BOL}}(1400\text{\AA})$ to a constant value of 2-3 at large AGN luminosity and large M_{BH} . The small range in k_{BOL} is due to the combination of the small $L_{\text{ION}}/L_{\text{AGN}}$ typical of such sources, and the restrictions imposed here on L/L_{Edd} . For the range of BH spin and L/L_{Edd} allowed here,

$$\log L_{\text{ION}} \simeq 12.9 + 0.72 \log L(1400\text{\AA}). \quad (4)$$

For $L(1400\text{\AA}) > 10^{47} \text{ erg s}^{-1}$, L_{ION} is considerably smaller than L_{AGN} and its exact value, which is sensitive to the exact value of a and M_{BH} , does not influence much the derived k_{BOL} .

An important potential source of uncertainty in $k_{\text{BOL}}(2-10 \text{ keV})$ is the unknown radiation pattern of the X-ray corona. In this work I assumed isotropic X-ray emission. This means that $k_{\text{BOL}}(2-10 \text{ keV})$ is the same for type-I and type-II AGN. An X-ray radiation pattern similar to a thin disk pattern would result in a larger $k_{\text{BOL}}(2-10 \text{ keV})$ for type-II sources. There are other implications to the X-ray radiation pattern like those discussed in Netzer (1987).

Finally, Fig. 2 and Fig. 4 suggest that $\text{EW}(\text{H}\beta)$, and the equivalent widths of other narrow emission lines, such as $[\text{O III}] \lambda 5007$, are much smaller in high luminosity, large BH mass sources, provided the NLR covering factor is not increasing with luminosity. There are indications that this is indeed observed in the most luminous AGN (e.g. Shemmer et al. 2004; Netzer et al. 2004), although other explanations (an NLR size that exceeds the size of the host galaxy) have been proposed.

4 CONCLUSIONS

Optically thick geometrically thin ADs are likely to be the powerhouse of many AGN. The case of a disk which extends all the way to the ISCO allows simple, straight-forward computations of various bolometric correction factors that enable more robust estimates of L_{AGN} that are not sensitive to the details of the X-ray production mechanism. Such approximations are superior to various constant bolometric correction factors used in the literature.

The new calculations provide simple approximations for $k_{\text{BOL}}(5100\text{\AA})$, $k_{\text{BOL}}(3000\text{\AA})$ and $k_{\text{BOL}}(1400\text{\AA})$ for type-I AGN, and $k_{\text{BOL}}(2-10 \text{ keV})$ and $k_{\text{BOL}}(\text{H}\beta)$ for both types of AGN, excluding LINERs, over a large range of BH mass, BH spin and BH accretion rate. Their use can lead to a better evaluation of L_{AGN} and L/L_{Edd} in various situations of astrophysical interest. The paper demonstrates the large inherited uncertainty in estimating L_{AGN} in cases where the BH spin and accretion rate are not known. The unknown inclination of the disk in type-I AGN is an additional source of uncertainty. Previous knowledge of the BH mass can reduce this uncertainty considerably.

5 ACKNOWLEDGMENTS

I am grateful to Benny Trakhtenbrot for useful comments and suggestions. I also thank the referee, Chris Done, for comments and suggestions that helped to clarify the main points of this work.

REFERENCES

Beckmann, V. & Shrader, C. R. 2012, *Active Galactic Nuclei*

- Bertemes, C., Trakhtenbrot, B., Schawinski, K., Done, C., & Elvis, M. 2016, *MNRAS*, 463, 4041
- Campitiello, S., Ghisellini, G., Sbarato, T., & Calderone, G. 2018, *A&A*, 612, A59
- Capellupo, D. M., Netzer, H., Lira, P., Trakhtenbrot, B., & Mejía-Restrepo, J. 2015, *MNRAS*, 446, 3427
- . 2016, *MNRAS*, 460, 212
- Collin, S., Boisson, C., Mouchet, M., Dumont, A.-M., Coupé, S., Porquet, D., & Rokaki, E. 2002, *A&A*, 388, 771
- Davis, S. W. & Laor, A. 2011, *ApJ*, 728, 98
- Davis, S. W., Woo, J.-H., & Blaes, O. M. 2007, *ApJ*, 668, 682
- Done, C., Davis, S. W., Jin, C., Blaes, O., & Ward, M. 2012, *MNRAS*, 420, 1848
- Done, C., Jin, C., Middleton, M., & Ward, M. 2013, *MNRAS*, 434, 1955
- Du, P., Hu, C., Lu, K.-X., Huang, Y.-K., Cheng, C., Qiu, J., Li, Y.-R., Zhang, Y.-W., Fan, X.-L., Bai, J.-M., Bian, W.-H., Yuan, Y.-F., Kaspi, S., Ho, L. C., Netzer, H., Wang, J.-M., & SEAMBH Collaboration. 2015, *ApJ*, 806, 22
- Heckman, T. & Best, P. 2014, *ArXiv e-prints*
- Heckman, T. M., Kauffmann, G., Brinchmann, J., Charlot, S., Tremonti, C., & White, S. D. M. 2004, *ApJ*, 613, 109
- Hryniewicz, K., Czerny, B., Nikolajuk, M., & Kuraszkiewicz, J. 2010, *MNRAS*, 404, 2028
- Jin, C., Ward, M., & Done, C. 2012a, *MNRAS*, 422, 3268
- . 2012b, *MNRAS*, 425, 907
- Just, D. W., Brandt, W. N., Shemmer, O., Steffen, A. T., Schneider, D. P., Chartas, G., & Garmire, G. P. 2007, *ApJ*, 665, 1004
- Krawczyk, C. M., Richards, G. T., Mehta, S. S., Vogeley, M. S., Gallagher, S. C., Leighly, K. M., Ross, N. P., & Schneider, D. P. 2013, *ApJS*, 206, 4
- Kubota, A. & Done, C. 2018, *MNRAS*, 480, 1247
- Laor, A. & Davis, S. W. 2011, *MNRAS*, 417, 681
- . 2014, *MNRAS*, 438, 3024
- Laor, A., Netzer, H., & Piran, T. 1990, *MNRAS*, 242, 560
- Lusso, E. & Risaliti, G. 2016, *ApJ*, 819, 154
- Lusso, E., Worseck, G., Hennawi, J. F., Prochaska, J. X., Vignali, C., Stern, J., & O'Meara, J. M. 2015, *MNRAS*, 449, 4204
- Marconi, A., Risaliti, G., Gilli, R., Hunt, L. K., Maiolino, R., & Salvati, M. 2004, *MNRAS*, 351, 169
- Mejía-Restrepo, J. E., Trakhtenbrot, B., Lira, P., Netzer, H., & Capellupo, D. M. 2016, *MNRAS*, 460, 187
- Mineshige, S., Kawaguchi, T., Takeuchi, M., & Hayashida, K. 2000, *PASJ*, 52, 499
- Narayan, R. 2005, *Ap&SS*, 300, 177
- Nemmen, R. S. & Brotherton, M. S. 2010, *MNRAS*, 408, 1598
- Netzer, H. 1987, *MNRAS*, 225, 55
- . 2009, *ApJ*, 695, 793
- . 2013, *The Physics and Evolution of Active Galactic Nuclei*
- Netzer, H., Lani, C., Nordon, R., Trakhtenbrot, B., Lira, P., & Shemmer, O. 2016, *ApJ*, 819, 123
- Netzer, H., Shemmer, O., Maiolino, R., Oliva, E., Croom, S., Corbett, E., & di Fabrizio, L. 2004, *ApJ*, 614, 558
- Netzer, H. & Trakhtenbrot, B. 2014, *MNRAS*, 438, 672
- Panda, S., Czerny, B., Done, C., & Kubota, A. 2019, *ApJ*, 875, 133
- Pennell, A., Runnoe, J. C., & Brotherton, M. S. 2017, *MNRAS*, 468, 1433
- Reynolds, C. S. 2016, *Astronomische Nachrichten*, 337, 404
- Ricci, C., Trakhtenbrot, B., Koss, M. J., Ueda, Y., Del Vecchio, I., Treister, E., Schawinski, K., Paltani, S., Oh, K., Lamperti, I., Berney, S., Gandhi, P., Ichikawa, K., Bauer, F. E., Ho, L. C.,

- Asmus, D., Beckmann, V., Soldi, S., Baloković, M., Gehrels, N., & Markwardt, C. B. 2017, *ApJS*, 233, 17
- Richards, G. T., Lacy, M., Storrie-Lombardi, L. J., Hall, P. B., Gallagher, S. C., Hines, D. C., Fan, X., Papovich, C. J., Berk, D. E. V., Trammell, G. B., Schneider, D. P., Vestergaard, M., York, D. G., Jester, S., Anderson, S. F., Budavari, T., & Szalay, A. S. 2006, *The Astrophysical Journal Supplement Series*, 166, 52
- Runnoe, J. C., Brotherton, M. S., & Shang, Z. 2012a, *MNRAS*, 422, 478
- . 2012b, *MNRAS*, 426, 2677
- Sądowski, A., Abramowicz, M., Bursa, M., Kluźniak, W., Lasota, J.-P., & Różańska, A. 2011, *A&A*, 527, A17
- Sądowski, A. & Gaspari, M. 2017, *MNRAS*, 468, 1398
- Sądowski, A. & Narayan, R. 2016, *MNRAS*, 456, 3929
- Shakura, N. I. & Sunyaev, R. A. 1973, *A&A*, 24, 337
- Shemmer, O., Netzer, H., Maiolino, R., Oliva, E., Croom, S., Corbett, E., & di Fabrizio, L. 2004, *ApJ*, 614, 547
- Shen, Y., Richards, G. T., Strauss, M. A., Hall, P. B., Schneider, D. P., Snedden, S., Bizyaev, D., Brewington, H., Malanushenko, V., Malanushenko, E., Oravetz, D., Pan, K., & Simmons, A. 2011, *ApJS*, 194, 45
- Slone, O. & Netzer, H. 2012, *MNRAS*, 426, 656
- Trakhtenbrot, B. & Netzer, H. 2012, *MNRAS*, 427, 3081
- Vasudevan, R. V. & Fabian, A. C. 2007, *MNRAS*, 381, 1235